Phase sequences and long-range interactions in ferroelectric liquid crystals

M. B. Hamaneh and P. L. Taylor*
Department of Physics, Case Western Reserve University, Cleveland, Ohio 44106-7079, USA
(Received 25 January 2005; published 17 August 2005)

The origin of the long-range interlayer interactions responsible for the variety of phases exhibited by ferroelectric liquid crystals is discussed. It is shown that the anisotropy of the elastic constants that govern layer bending in smectic-*C* liquid crystals results in an effective long-range interaction between the smectic layers. The nature of this interaction is such as to favor a mutual alignment of the *c* directors of the layers in either a parallel or antiparallel orientation. The free energy of the system is the sum of the contributions of these long-range interlayer interactions and the short-range interaction between nearest-neighboring layers, which favors a purely helical structure for the *c* directors. The long-range interaction is found to favor commensurate structures while the short-range term favors incommensurate helices. The resulting structure is of the type characterized in the "distorted clock model." The phase diagrams that result from the application of this theory are consistent with the experimentally observed phase sequences.

DOI: 10.1103/PhysRevE.72.021706 PACS number(s): 61.30.Cz

I. INTRODUCTION

One of the most remarkable properties of smectic liquid crystals is the wide variety of phases that can arise as the temperature is varied over a comparatively narrow range. Some of these phases display ordering phenomena in which the average orientation of the molecules in one smectic layer appears to be correlated with the orientation in a comparatively distant layer. This implies the existence of a long-range interaction between these layers. The origin and nature of this interaction has been one of the most long-standing puzzles in the physics of liquid crystals.

Very recently a mechanism has been proposed that appears capable of giving rise to a long-range interlayer interaction [1]. In this paper we expand upon the brief account given previously, and point out some of the strengths and weaknesses of the underlying theory. We also indicate the type of phase sequence that can be predicted on the basis of this type of mechanism, and hence the type of phase sequence that would lie outside the range of possible predictions. This is of interest, as any experimental result indicating the existence of such a phase sequence would cast doubt on the adequacy of the model as a basis for a complete description of phase transitions in ferroelectric liquid crystals.

We begin by establishing the notation used to describe smectic liquid crystals, in which rod-shaped molecules are arranged in layers. In the case of the smectic-*A* phase the average molecular orientation is along the layer normal, which we take as defining the *z* axis. The system is then isotropic in the *x*-*y* plane. In the smectic-*C* phase, on the other hand, the molecules are tilted from the layer normal. This tilt identifies a unique direction in the *x*-*y* plane, along which the *c* director is said to lie. Of particular interest are the smectic-C^* phases that can arise when the liquid crystal consists of chiral molecules, as in these materials the *c* director may vary from layer to layer. If we denote the angle between the *c* director and the *x* axis in the *l*th smectic layer as ϕ_l, we may characterize the system in terms of how ϕ_l changes with increasing *l*. When ϕ_l remains constant we have a synclinic phase, while when it increases by π per layer the phase is anticlinic. The presence of a transverse permanent electric dipole moment leads to the alternative description of these phases as ferroelectric and antiferroelectric. If the sample geometry permits, there may also be a small constant increment per layer, giving the structure a helically varying electric polarization. In the materials with which we are concerned, there is an even richer structure, with ϕ_l increasing by approximately 2π every three or four layers (the so-called ferrielectric or intermediate phases), or advancing in an incommensurate manner.

A wide variety of sequences of phases has been observed as the temperature is raised from the melting point through the various smectic phases [2,3]. One example has the sequence Sm-C_A^* (antiferroelectric) – Sm-C_{FI1}^* (intermediate) – Sm-C_{FI2}^* (intermediate) – Sm-C^* (ferroelectric) – Sm-C_α^* (incommensurate) – Sm-*A* [4]. In other materials, one or more of these phases may be missing, but the ordering generally follows in the same sequence. This suggests a common origin in the underlying mechanism responsible for the existence of the various phases. We shall see that the possible sequences are determined by the topology of a map in which the stable phases appear as areas in a plot in which the properties of the nearest-layer interaction and the long-range interaction are represented along the two axes.

Previous attempts to find a mechanism for interlayer interactions have been mostly guided by perceptions held about the nature of the layer structure at the time the particular theory was developed. Before recent observations had clarified the nature of the variation of ϕ_l with *l*, two different models had been proposed to describe the molecular arrangement in these materials. In the Ising-like model [5–7], $\Delta\phi_l \equiv \phi_{l+1} - \phi_l$ is restricted to be either 0 or π, while in the clock model [8–11] $\Delta\phi_l = 2\pi/n$, where *n* is the number of the layers in the repeating unit cell, namely, 1 for ferroelectric, 2 for antiferroelectric, and 3 or 4 for the intermediate phases. Recent experiments [12–14] have ruled out both the Ising-like

*Electronic address: taylor@case.edu

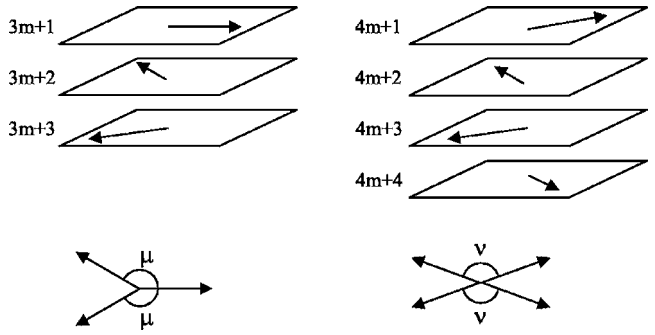

FIG. 1. In the distorted clock model, structures with a periodicity of three or four layers can each be defined by a single angle μ or ν.

model and the pure clock model, and led to the introduction of the so-called distorted clock model [15–20]. As indicated in Fig. 1, in this model a system with three-layer periodicity has $\Delta\phi_{3m+1}=\Delta\phi_{3m+3}=\mu$, and $\Delta\phi_{3m+2}=2(\pi-\mu)$, while a system with four layers in a unit cell can be characterized by $\Delta\phi_{4m+1}=\Delta\phi_{4m+3}=\nu$, and $\Delta\phi_{4m+2}=\Delta\phi_{4m+4}=\pi-\nu$ with $m=0,1,2,\ldots$. The measured values for μ and ν are closer to π than to the expected values in a pure commensurate helix ($2\pi/3$ and $\pi/2$ for three-layer and four-layer unit cells, respectively), which means that the observed structures are a large distortion of the clock model.

A structure in which the angle ϕ_l at large l is uncorrelated with its value at $l=0$ is said to be incommensurate. This type of structure arises when the only interaction is between nearest-neighbor layers. If the interaction energy is minimized when $\Delta\phi_l$ is equal to some angle α, then the ground state will be a nonrepeating helical structure when α is an irrational fraction of 2π. Even if α is a rational fraction of 2π, at finite temperatures long-range order will be lost. In order to have the system form a commensurate helix, in which ϕ_l is correlated over large distances, some type of competing interaction of longer range is required.

The many papers that discuss the formation of the various phases can be divided into two groups. The small number of papers in the first group derive the form of the interlayer interactions from first principles, and then proceed to investigate the resulting phase sequences. The much larger second category comprises papers of a phenomenological nature, in which some type of second-nearest-neighbor or higher-order interaction is assumed without explicit derivation. Having assumed that longer-range interactions do exist, these authors then explored the consequent phase diagram. In some models the system is described by the tilt vectors $\boldsymbol{\xi}_l=\theta_l\mathbf{c}_l$, where $\mathbf{c}_l$ and θ_l are the c director and the molecular tilt angle, respectively, in the lth layer. Dolganov *et al.* [17,18] have proposed a model in which only the nearest-neighbor and next-nearest-neighbor interactions are taken into account. The interlayer part of their free energy is given by

$$\mathcal{F}=\sum_l\left(\sum_{i=1}^{2}a_i\boldsymbol{\xi}_l\cdot\boldsymbol{\xi}_{l+i}+f\boldsymbol{\xi}_l\times\boldsymbol{\xi}_{l+1}+a_3(\boldsymbol{\xi}_l\times\boldsymbol{\xi}_{l+1})^2+b\boldsymbol{\xi}_l^2(\boldsymbol{\xi}_l\cdot\boldsymbol{\xi}_{l+1}+\boldsymbol{\xi}_{l-1}\cdot\boldsymbol{\xi}_l)\right). \quad (1)$$

According to these authors, the fact that the layer tilt angle θ can vary from layer to layer results in stable intermediate phases without the need for consideration of longer-range interactions. Čepič *et al.* [9,16], on the other hand, proposed a phenomenological model in which the polarization induced by piezoelectric and flexoelectric effects is taken into account, resulting in the free energy

$$\mathcal{F}=\sum_l\left(\sum_{i=1}^{4}a_i\boldsymbol{\xi}_l\cdot\boldsymbol{\xi}_{l+i}+\sum_{i=1}^{3}f_i\boldsymbol{\xi}_l\times\boldsymbol{\xi}_{l+i}+b(\boldsymbol{\xi}_l\cdot\boldsymbol{\xi}_{l+1})^2\right). \quad (2)$$

The third- and fourth-nearest-neighbor interactions arise indirectly from a short-range interaction between the tilt vector and an independently varying polarization vector when electrostatic fluctuation forces are included.

Bruinsma and Prost [21] have discussed several candidate mechanisms for a long-range interaction, but dismiss most of these as vanishing or insignificant. They determine, for example, the contribution due to thermal elastic fluctuations in the c director by invoking a pseudo-Casimir effect [22–24]. Finding this to be weak, they then concentrate on the electrostatic effect of thermal fluctuations, $\delta\phi_l(x,y)$, in ϕ_l within a layer. They calculate an interaction between layers arising from the effective charge density produced by in-plane variation in $\delta\phi_l(x,y)$ and hence in the electric polarization, and suggest that this may induce a tendency to anticlinic ordering in distant layers. Their work was performed at a time when the Ising model was favored as a description of ferroelectric liquid crystals, and so they did not go on to suggest any mechanism that could lead to more complex structures.

Our goal in the present paper is to present in detail a physical model that can be shown to give rise to long-range interlayer interactions, and from which the distorted clock structure of the various phases can be derived [1]. The essential ingredient is a mechanism that induces the c directors in nonadjacent layers to align in a parallel or antiparallel direction. The origin of the mechanism we propose is the anisotropy in stiffness of a single layer of Sm-C^* material [25]. If a layer is bent by curving it around a cylinder whose axis is along the c director, then the restoring force will be related mostly to the strength of the splay elastic constant. If, on the other hand, it is bent in the perpendicular direction then the restoring force will depend on a mixture of splay and bend elastic constants. The elastic properties of the assembly of layers that forms the Sm-C^* liquid crystal will then be different for a system in which the c directors of all the layers have some preferred alignment from the properties of a liquid crystal with no preferred c director orientation.

We can give a physical picture of the free energy we propose by making an analogy with a sheet of plywood, which is made from alternating layers of wood veneer. For maximum stiffness of the composite material, the grain of the wood in each layer is arranged to be perpendicular to that in its neighboring layers, as illustrated in Fig. 2. When subject to random oscillations, the amplitude of vibrations is then minimized. In thermodynamic terms, the amount of phase space occupied, and hence the entropy, is also minimized by making the direction of the grain of the wood in each layer perpendicular to that of its neighbor. Now suppose

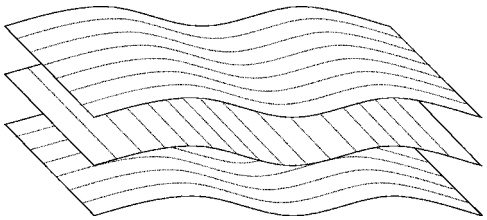

FIG. 2. Plywood analogy for Sm-C^* liquid crystals: The stiffness of each individual layer is least along its c director, and the average stiffness of the composite system of N layers is least when all the c directors are parallel.

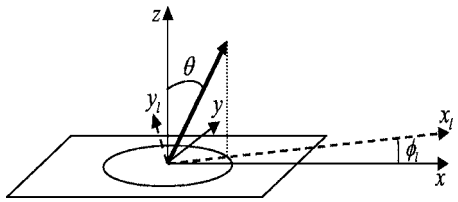

FIG. 3. In each smectic layer the c director lies in the x-y plane at an angle ϕ_l to the x axis. The ϕ_l in different layers are coupled by direct short-range interactions and indirect long-range interactions.

that we lift the constraint on perpendicular orientation, and allow the various layers to rotate in their own planes. In order to maximize the entropy, the system will tend to move towards the configuration where the average stiffness is least, which will be when all layers have their grain direction parallel. In the case of a Sm-C^* liquid crystal, an arrangement where all the c directors are parallel or antiparallel will similarly maximize the entropy, and will be the preferred arrangement in the absence of other forces.

II. MODEL

In order to be capable of supporting a variety of commensurate and incommensurate phases, a model must have two components. The first of these is a short-range interaction that typically favors a particular relationship between nearest neighbors. This is usually a tunable term whose nature varies with some control parameter, such as temperature or pressure. The second component is a longer-range interaction, which favors a structure different from that preferred by the short-range forces.

The short-range interaction V_{sr} acting between adjacent layers is easy to visualize, as the molecules are in physical contact. It is, however, difficult to calculate from first principles. For this reason we shall make no attempt to derive this term, but simply assume it to favor a particular value of $\Delta\phi$, the angle between c directors in successive layers. As a simple example, for layers of area L^2 we initially choose the simple form

$$V_{\mathrm{sr}} = -vL^2 \sum_l \cos(\phi_{l+1} - \phi_l - \alpha), \tag{3}$$

with the parameter v being an energy of interaction per unit area. This term favors the formation of a helical ordering in which $\phi_l = \mathrm{const} + l\alpha$. We assume that α varies with temperature T from a value near zero to a value near π as the temperature is lowered through the range in which the multiple smectic-C^* phases are found.

There is no explicit microscopic model for this variation, but its existence can be argued as plausible. It becomes clear that it is not feasible to develop a microscopic model for the form of $\alpha(T)$ when one considers some recent measurements by Cady *et al.* [26] of the pitch of the helix in the incommensurate Sm-C^*_α phase. There it was found that the addition of one extra CH_2 group to the achiral alkyl chain of the large molecule 10-OHFBBB1M7 had a dramatic effect on the pitch of the helix. It not only changed the pitch by an order of magnitude, but also changed the sign of its temperature dependence. In terms of our model, the sign of $d\alpha/dT$ was reversed. This makes it unlikely that any simple structural model can lead to reliable predictions of $\alpha(T)$. It is, however, perfectly reasonable to imagine that the mutual contact of molecules in adjacent layers should give rise to some well-defined interaction V_{sr}, even if its form cannot be predicted.

The longer-range interaction is the more difficult to establish, as discussed in the previous section. The absence of direct contact between distant layers requires the invocation of an indirect interaction. The mechanism we propose is the contribution to the free energy from the anisotropy in the force required for the physical bending of a layer in a smectic-C liquid crystal. This anisotropy causes the energy of distortion of two neighboring layers to depend on the extent to which their c directors are aligned. The spontaneous thermal fluctuations in shape of a layer give contributions to the entropy of the system that reflect the degree of alignment. This effective long-range elastic interaction is strong enough to induce commensurate ordering.

We define our model as consisting of N layers of thickness d in a Sm-C^* liquid crystal of density ρ. In the absence of thermal fluctuations, each layer lies in the x-y plane, as shown in Fig. 3. The director in each layer is assumed to be tilted away from the layer normal by a tilt angle θ that is a constant throughout the sample. The angle ϕ_l between the c director of the lth layer and the x axis is initially assumed to be uniform within each layer, and so does not depend on x or y. Different layers, however, have different ϕ's. Thermal fluctuations then cause a spatially varying displacement $u_l(x,y)$ of the lth layer in the z direction. The dynamic variables in terms of which the system is defined are then the N angles ϕ_l and the N functions $u_l(x,y)$.

It is convenient to define a local coordinate system aligned with the c director in which to write the expression for the elastic energy of each layer. If x_l is an axis in the direction of the c director in the lth layer and y_l is the perpendicular axis in the x-y plane, one can write the elastic energy per unit area of this layer as [25,27]

$$f_l = \frac{1}{2}A_{12}\left(\frac{\partial^2 u_l}{\partial x_l^2}\right)^2 + \frac{1}{2}A_{21}\left(\frac{\partial^2 u_l}{\partial y_l^2}\right)^2 + A_{11}\left(\frac{\partial^2 u_l}{\partial y_l\,\partial x_l}\right)^2 \tag{4}$$

where A_{12}, A_{21}, and A_{11} are the elastic constants for bending the layer in different directions. By specifying a single angle ϕ_l to define the orientation of the c director for an entire layer we are implicitly making the assumption that local

fluctuations in ϕ_l within a layer are unimportant. Such fluctuations do occur, but are large only when the system is close to making a transition from being a smectic-C material to being smectic-A. We shall find that in this region the long-range interactions are absent, causing the liquid crystal to form an incommensurate helix, and making the in-layer fluctuations irrelevant.

Because the displacements $u_l(x,y)$ in the z direction differ from layer to layer, we must include in the total elastic energy of the system a contribution due to the compression or expansion of the thickness of a layer. We associate an elastic constant k with this compression energy. When we also include the kinetic energy of layer motion, the total effective Hamiltonian of the system is then of the form

$$\mathcal{H} = V_{\rm sr} + \sum_{l=1}^{N} \int\int \left[f_l + \frac{1}{2}k(u_{l+1}-u_l)^2 + \frac{1}{2}\rho d\left(\frac{\partial u_l}{\partial t}\right)^2 \right] dx_l\, dy_l. \tag{5}$$

Our approach now is to find the set of values of the macroscopic variables ϕ_l that minimize the free energy of the system. We can do this in two equivalent ways. The most direct method is simply to evaluate the partition function for this Hamiltonian, in which case the kinetic-energy term in Eq. (5) is unimportant. The alternative approach is to analyze the motion governed by the Hamiltonian into normal modes of vibration of frequency ω, and then attribute an entropy $-k_B \ln \omega$ to each mode. This latter approach has the great advantage of giving a clear physical picture of the phenomenon. It also allows one to include the effects of the damping of the normal modes of oscillation that arises from the viscous nature of liquid crystals. The entropy of a damped harmonic oscillator has been shown [28] to be the convolution of $-k_B \ln \omega$ with a function that represents the broadening of the oscillator resonance. The partition-function approach does not lend itself so readily to the inclusion of dissipative effects. We accordingly first find the normal modes of excitation of the microscopic variables $u_l(x,y)$ for a given set of fixed values for the ϕ_l. We then add the contribution to the free energy from these thermal excitations to the short-range potential energy, and minimize this total. Because the frequencies of the normal modes themselves depend on the ϕ_l, this is a self-consistent procedure.

The boundary conditions encountered in the most common experimental situations are quite complex. These range from strong anchoring at a solid substrate to weak anchoring at a liquid crystal-air interface in free-standing films. To avoid these difficulties, we consider a system that is sufficiently large that we do not introduce significant error by assuming periodic boundary conditions. For a given set of fixed values for the ϕ_l in a sample of thickness Nd and layer area L^2, we write

$$u_l(x,y,t) = \sum_{\mathbf{q}} u_{\mathbf{q}} \exp i(q_x x + q_y y + q_z l d). \tag{6}$$

Here $q_x = 2\pi n_x/L$, $q_y = 2\pi n_y/L$, and $q_z = 2\pi n_z/Nd$. This transformation diagonalizes the Hamiltonian for wave-number components lying in the x-y plane, but leaves interactions between modes of different q_z, so that

$$\begin{aligned}\mathcal{H} = V_{\rm sr} &+ \frac{1}{2}NL^2\rho d \sum_{\mathbf{q}} \frac{\partial u_{\mathbf{q}}}{\partial t}\frac{\partial u_{-\mathbf{q}}}{\partial t} \\ &+ \frac{1}{2}NL^2 k \sum_{\mathbf{q}} 2(1-\cos q_z d) u_{\mathbf{q}} u_{-\mathbf{q}} \\ &+ \frac{1}{2}L^2 \sum_{\mathbf{q},q_z'} u_{q_x,q_y,q_z} u_{-q_x,-q_y,-q_z'} \sum_l (A_{12} q_{x_l}^4 + 2A_{11} q_{x_l}^2 q_{y_l}^2 \\ &+ A_{21} q_{y_l}^4) \\ &\times \exp[ild(q_z - q_z')]\end{aligned} \tag{7}$$

where

$$q_{x_l} = q_x \cos\phi_l + q_y \sin\phi_l \quad \text{and} \quad q_{y_l} = -q_x \sin\phi_l + q_y \cos\phi_l. \tag{8}$$

This may be simplified by introducing the angle φ between the x axis and the component of $\mathbf{q}$ in the x-y plane, whose magnitude we write as $q_\perp$, and in terms of which

$$q_x = q_\perp \cos\varphi \quad \text{and} \quad q_y = q_\perp \sin\varphi. \tag{9}$$

The sum over l in Eq. (7) then becomes

$$\begin{aligned}\sum_l q_\perp^4 \Big(&\bar{A} + \frac{1}{2}\Delta A_1 \cos(2\phi_l - 2\varphi) \\ &+ \frac{1}{4}\Delta A_2 \cos(4\phi_l - 4\varphi) \Big) \exp[ild(q_z - q_z')],\end{aligned} \tag{10}$$

with $\bar{A} \equiv \frac{1}{8}[3(A_{12}+A_{21})+2A_{11}]$, $\Delta A_1 \equiv A_{12}-A_{21}$, and $\Delta A_2 \equiv (A_{12}+A_{21})/2 - A_{11}$.

The dominant terms in this sum will be the diagonal ones, for which $q_z = q_z'$, and which have their origin in the nonoscillatory factor $\bar{A}$. The off-diagonal terms arise when the factors $\cos(2\phi_l - 2\varphi)$ and $\cos(4\phi_l - 4\varphi)$ exhibit the same spatial periodicity as the exponential factor. For example, for a purely helical structure, for which ϕ_l would be just $l\alpha$, scattering terms would exist whenever $q_z - q_z' = 2(m\pi \pm \alpha)/d$. Here m is an integer for which a nonzero value corresponds to so-called umklapp scattering, in which conservation of wave number occurs only when a reciprocal lattice vector is included in the equation. The effect of such terms is to introduce gaps into the dispersion relation for the normal mode frequency $\omega_{\mathbf{q}}$ as a function of q_z. If α were equal to $2\pi/3$, for example, which would correspond to a three-layer repeat in the undistorted clock model, then band gaps would open at $q_z = \pm\pi/3d$ and $q_z = \pm 2\pi/3d$.

The off-diagonal terms can be treated using the standard methods of the theory of solids [29], but for detailed calculations of specific systems it is in practice more convenient to take a numerical rather than an analytical approach, and revert to a real-space formulation for dealing with these terms. This has the advantage of being more flexible, in that it can handle systems like free-standing films, for which the boundary conditions must be modified. It also yields a more direct physical picture of the range of the interlayer interactions.

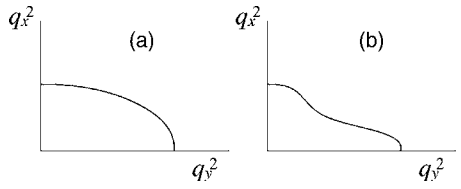

FIG. 4. Increasing the term ΔA_2 modifies the contour of constant frequency ω from an ellipse (a) to a higher-order curve (b).

For the purposes of illustrating the effects of the interlayer interactions, however, we make a mean-field approximation by using the wave-number-space formalism and retaining only the diagonal terms. We bear in mind that this approximation significantly overestimates the effect of the interactions, as it includes a self-energy term related to the anisotropy of a single layer and also includes nearest-neighbor interactions, whose inclusion is equivalent to a modification of $V_{\rm sr}$. We follow this path in order to develop the broad picture of the commensurate-incommensurate transition, which is not so easily visualized in the real-space formulation.

With this decision to retain only the diagonal terms, the sum in Eq. (10) reduces to

$$\sum_l q_\perp^4 \left(\bar{A} + \frac{1}{2}\Delta A_1 \cos(2\phi_l - 2\varphi) + \frac{1}{4}\Delta A_2 \cos(4\phi_l - 4\varphi) \right). \tag{11}$$

The sums over $\cos(2\phi_l - 2\varphi)$ and $\cos(4\phi_l - 4\varphi)$ will vanish unless the symmetry of the helical arrangement of the ϕ_l is broken. It is easy to see how the sum over $\cos(2\phi_l - 2\varphi)$ could be nonvanishing, as each layer has an axis of easy bending and an axis along which bending requires greater energy. If there is some tendency to mutual alignment of the easy axes of all the layers, then the greater amplitude of thermal bending that this permits will reduce the free energy of the system, and the tendency to alignment will be self-sustaining if the coefficient ΔA_1 is sufficiently large.

It is less clear how a nonvanishing sum over $\cos(4\phi_l - 4\varphi)$ could arise. This would require a fourfold axis of easy bending of each layer, and a correlation between layer orientations that would retain this property in the whole sample. While this is not forbidden by any general symmetry requirement, it would represent an unusual mechanical property for a single layer. One would expect to find an axis of easy bending either along the c director or perpendicular to it, and not at some angle approaching ±45° from it. We can visualize this unusual situation by plotting contours of constant ω at $q_z = 0$ in the q_x^2-q_y^2 plane. The lowest-order curve would be an ellipse, as shown in Fig. 4(a), and this would arise if A_{11} were the geometric mean of A_{12} and A_{21}. The coefficient ΔA_2 vanishes when A_{11} is the arithmetic mean of A_{12} and A_{21}, and since the difference between A_{12} and A_{21} is comparatively small the geometric and arithmetic means will almost coincide, making ΔA_2 very small. To obtain a significant value for ΔA_2 would require a large distortion of the contour of constant ω to something resembling Fig. 4(b). There are no direct measurements of this coefficient, but some related experimental results [30] suggest that $A_{12} > A_{11} > A_{21}$, which implies that ΔA_2 is significantly smaller than ΔA_1, and would exclude a situation such as that shown in Fig. 4(b). We will consequently assume this term to be too weak to reach the threshold for symmetry breaking, and will ignore this contribution in the following calculations.

This leaves us with the term in $\cos(2\phi_l - 2\varphi)$ as the component of the Hamiltonian relevant for long-range interlayer interactions. At this point it is convenient to choose our coordinate system so that the symmetry is broken in such a way that the distribution of the ϕ_l is symmetric about the x axis, causing sums like $\Sigma_l \sin 2\phi_l$ to vanish. The order parameter for the symmetry breaking is then

$$J \equiv N^{-1} \sum_l \cos 2\phi_l. \tag{12}$$

This quantity will vanish for the helical distribution of the ϕ_l characteristic of the pure clock model, but will be nonzero in the distorted clock arrangement. In terms of this parameter the Hamiltonian is

$$\mathcal{H} = V_{\rm sr} + \frac{1}{2} N L^2 \sum_{\mathbf{q}} \left(\rho d \frac{\partial u_{\mathbf{q}}}{\partial t} \frac{\partial u_{-\mathbf{q}}}{\partial t} + [2k(1 - \cos q_z d) + q_\perp^4 \bar{A}(1 + \Gamma J \cos 2\varphi)] u_{\mathbf{q}} u_{-\mathbf{q}} \right). \tag{13}$$

Here we have introduced the layer anisotropy parameter $\Gamma \equiv \Delta A_1 / 2\bar{A}$. The dispersion relation of the normal-mode frequencies is then

$$(\rho d/k)\omega_{\mathbf{q}}^2 = 4 \sin^2(q_z d/2) + (q_\perp d)^4 g(\varphi, J), \tag{14}$$

where $g(\varphi, J) \equiv c(1 + \Gamma J \cos 2\varphi)$ with $c \equiv \bar{A}/kd^4$. Because the low-frequency modes are dominant, a Debye-like approximation can be made in which $\sin q_z d$ can be replaced by $q_z d$, and

$$(\rho d/k)\omega_{\mathbf{q}}^2 = (q_z d)^2 + (q_\perp d)^4 g(\varphi, J). \tag{15}$$

III. FREE ENERGY

We are now in a position to form an expression for the free energy of the system as a function of the ϕ_l. The contribution from the normal modes in the absence of damping will be

$$\mathcal{F}_\omega = k_B T \sum_{\mathbf{q}} \ln \omega_{\mathbf{q}} = \frac{N d L^2 k_B T}{8\pi^3} \int_0^{\pi/d} dq_z \int_0^{\pi/d} q_\perp dq_\perp \int_0^{2\pi} d\varphi \ln \omega_{\mathbf{q}}^2. \tag{16}$$

The upper limit for the integration over $q_\perp$ is chosen to be about the reciprocal of the layer thickness, since distinct modes will not exist when the wavelength approaches molecular dimensions. Inclusion of damping increases the entropy slightly, and hence reduces the free-energy contribution [28].

Our interest in this expression centers on its dependence on the order parameter J, and so we drop unimportant con-

stant terms and integrate over q_z and $q_\perp$ to find

$$\mathcal{F}_\omega = \frac{NL^2k_BT}{16d^2}\int_0^{2\pi} d\varphi\left[\frac{1}{\pi\sqrt{g(\varphi,J)}}\arctan(\pi\sqrt{g(\varphi,J)}) + \ln[1+\pi^2 g(\varphi,J)] + \pi\sqrt{g(\varphi,J)}\arctan\left(\frac{1}{\pi\sqrt{g(\varphi,J)}}\right)\right]. \quad (17)$$

Since the anisotropy parameter Γ is small, $\mathcal{F}_\omega$ can be expanded as a power series in Γ. To lowest order, this part of the free energy has the form

$$\mathcal{F}_\omega = -\frac{\pi}{32}\frac{NL^2k_BT}{d^2}\Gamma^2J^2f(\pi\sqrt{c}) \quad (18)$$

with

$$f(x) = \frac{3}{4}\left(1-\frac{1}{x}\arctan x\right)+\frac{1}{4}x\arctan\left(\frac{1}{x}\right). \quad (19)$$

The total free energy per unit volume can then be written as

$$\mathcal{F} = \frac{V_{\rm sr}+\mathcal{F}_\omega}{L^2Nd} = -\frac{v}{Nd}\sum_l[\cos(\phi_{l+1}-\phi_l-\alpha)+\eta J^2] \quad (20)$$

with $\eta = \pi k_BT\Gamma^2 f(\pi\sqrt{c})/32d^2v$, and with J as defined in Eq. (12).

This expression may be put in a more familiar form if we substitute for just one of the two factors of J to write

$$\mathcal{F} = -\frac{v}{Nd}\sum_l[\cos(\phi_{l+1}-\phi_l-\alpha)+\eta J\cos 2\phi_l]. \quad (21)$$

If we were to consider J as a constant in this expression, then we would have a variant of the well-known Frenkel-Kontorova problem [31]. In this system, the first term favors an incommensurate helix while the second favors a commensurate periodic structure in which the values of ϕ_l repeat exactly after l has increased by some integer known as the order of commensurability. A procedure for finding the values of ϕ_l that minimize $\mathcal{F}$ has been developed [32,33]. One differentiates Eq. (21) to find a set of relations that are transformed into two sets of coupled nonlinear difference equations by a procedure analogous to the area-preserving Taylor-Chirikov mapping [34]. It was found that for large values of ηJ the system is always commensurate; a plot of the average $\langle\Delta\phi\rangle$ against ηJ would then be the series of discontinuous horizontal lines known as a complete devil's staircase. For small ηJ the system was sometimes incommensurate, making the devil's staircase incomplete.

The problem presented by Eq. (21) is more complicated than the case where J was constant, since in our case J must be self-consistently determined. The distortion of the clock model must be sufficiently large that the resulting distorting field represented by the order parameter J should be self-sustained. If no nonzero value of J can be found, then the system reverts to the pure incommensurate helix in which $\Delta\phi=\alpha$. For any given value of α, the crucial control factor is thus the quantity η that describes the relative strengths of the long-range and short-range interactions between layers. There will be a critical value $\eta_c(\alpha)$, of order of unity, below which the structure is always incommensurate and above which it will be commensurate.

This can be illustrated for the special case where α is close to $\pi/2$ by using expression (20) to examine the J dependence of the free energy of the four-layer-repeat structure. We put $\alpha=\pi/2+\epsilon$ and write the angle ν defined in Fig. 1 for the periodicity-4 structure as $\nu=\pi/2+\delta$. Then

$$\mathcal{F} = -\frac{v}{d}(\cos\delta\cos\epsilon+\eta J^2). \quad (22)$$

Since in this case $J=\sin\delta\simeq\delta$, and $\cos\delta\simeq 1-\delta^2/2$ while $\cos\epsilon\simeq 1$, we find

$$\mathcal{F} \simeq -\frac{v}{d}\left[1+\left(\eta-\frac{1}{2}\right)J^2\right]. \quad (23)$$

When $\eta>1/2$, a nonzero value of J will lower the free energy, and the commensurate four-layer-repeat structure will form. If $\eta<1/2$, on the other hand, then J will vanish, and the incommensurate structure having $\phi_{l+1}-\phi_l=\pi/2+\epsilon$ will be stable.

This leads us to the crucial question of whether the proposed long-range interaction is sufficiently strong to give rise to commensurate phases. We have now seen that this is equivalent to asking whether or not η can be of order unity. We return to the definition $\eta=\pi k_BT\Gamma^2f(\pi\sqrt{c})/32d^2v$, and note that $c\sim 1$, since it is a ratio of elastic constants. Consequently, $f(\pi\sqrt{c})$ will also be of order unity. We estimate the anisotropy parameter Γ by noting that if the tilt angle θ could approach $\pi/2$, then the director would lie in the layer plane along the axis x_l. Consequently A_{21} would vanish, A_{11} would be small, and we would have $\Gamma\gtrsim 1$. If we suppose Γ to vary as $\sin^2\theta$, then for a typical tilt angle of 18° we would have $\Gamma\sim 0.1$. This means that we require k_BT/d^2v to be of order 1000 to have $\eta\sim 1$.

We can estimate the magnitude of the energy d^2v by considering the electric field strength E_0 necessary to switch a material of dipole moment per unit volume P_0 between phases. At this transition, the electrostatic energy per unit volume, P_0E_0, will be of the order of v/d. The switching field is of the order of 0.3×10^6 V/m [35], and the dipole moment per unit volume is probably around 7×10^{-4} C/m^2 [36]. We then deduce that for a layer thickness d of 3 nm, the energy d^2v will be around $P_0E_0d^3$, or about 5×10^{-24} J, making k_BT/d^2v about 1000 and $\eta\sim 1$. The magnitudes thus appear to be in the appropriate range for the proposed mechanism to be important.

IV. PHASE DIAGRAM

To have a complete picture of the phase structure of the smectic liquid crystal we need two pieces of information. The first of these is the map that identifies whether a system of given α and η is commensurate or incommensurate, and, if commensurate, its order of commensurability. This is obtained by a minimization of the free energy given in Eq. (20). The second piece of information is the form of the functions $\alpha(T)$ and $\eta(T)$ that characterize the short-range and long-

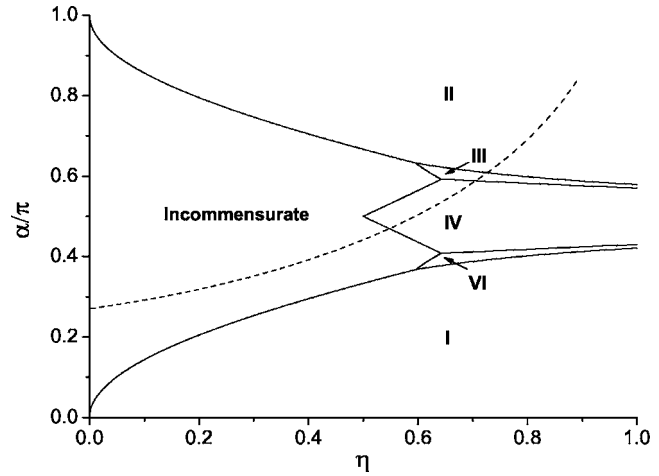

FIG. 5. This diagram shows the stable phases in a simple model as a function of the helix angle α (in radians) favored by nearest-neighbor interlayer interactions and of the dimensionless strength η of the mean-field long-range interaction. The Roman numerals labeling commensurate phases indicate the number of layers per repeat unit. The dashed line shows an experimentally observed phase sequence.

range interlayer interactions, respectively. From these one may form the function $\alpha(\eta)$ that traces the path of the system through the phases as the temperature is raised or lowered.

Solutions for the system defined by Eq. (20) were found by using a combination of analytical and numerical methods for all α and η. These results are shown in Fig. 5 for the case where the number N of layers is infinite, thereby eliminating the effects of the sample boundaries. Calculations were also performed for $N=50$ and with free boundary conditions in order to simulate the free-standing films used in many experiments. The results for free-standing films were found to be very similar to those for the infinite system when η is of order unity or larger. For small η the phase diagram is somewhat distorted, but the topology, and hence the predicted phase sequences, remains unchanged.

The first point one notices in Fig. 5 is that only a few commensurate phases exist in this model. This is in sharp distinction to the Frenkel-Kontorova model, in which J is a fixed parameter in Eq. (21). In that case there is an infinite number of commensurate phases, even when η is very small. In our model, in which J is a self-consistently determined mean field, there are no stable phases of order of commensurability higher than six. The six-layer periodicity, also predicted by Dolganov *et al.* [17,18], has not yet been observed experimentally.

In order to convert the phase diagram into a prediction of the sequence in which the different phases appear as the temperature is raised, we require knowledge of the function $\alpha(\eta)$, which can be obtained from $\alpha(T)$ and $\eta(T)$ if these are available. The main dependence of the long-range-interaction parameter η on T will come from its proportionality to Γ^2, since the anisotropy parameter Γ will vanish at the temperature of the transition to the Sm-A phase. As discussed previously, the dependence of α on T appears to be very sensitive to small details of the molecular structure, and so cannot be predicted. We expect the most common behavior to be a steady reduction from a value near π to a value near zero as the temperature is raised. The most common form of $\alpha(\eta)$ would then be a curve connecting the lower left of Fig. 5 to the upper right of the figure. The particular path followed then determines the phase sequence.

The dashed line shows one possibility for the form of $\alpha(\eta)$. As we move down the curve we pass from the antiferroelectric Sm-C_A^* phase, which has a two-layer repeat, to the intermediate Sm-C_{FI1}^* phase, which has a three-layer repeat. Raising the temperature further takes us into the second intermediate Sm-C_{FI2}^* phase, with its four-layer repeat. We then pass into the incommensurate Sm-C_α^* phase, in which η is too small to sustain the long-range interaction. Finally we reach the Sm-A phase represented by the vertical axis, along which $\eta=0$. This particular phase sequence has been observed in several materials, including the compound known as MHPBC [37,38]. Similar lines can be drawn to trace the path of the phase sequence Sm-C_A^*–Sm-C_α^*–Sm-A (compounds MHPOCBC [39] and TFMHPBC [40]) and Sm-C_A^*–Sm-A (compound EHPOCBC [6]).

Some experimentally observed phase sequences, however, cannot be accommodated by the phase diagram shown in Fig. 5. For example, some compounds exhibit a direct transition between the three-layer-repeat Sm-C_{FI1}^* phase and the ferroelectric Sm-C^* phase [4]. The fact that the four- and six-layer structures extend to infinite η in Fig. 5 clearly forbids this behavior. We accordingly need to ask which aspects of this figure are an artifact of the choice of $V_{\rm sr}$ and which are of a more general origin.

A noticeable feature of the phase diagram shown in Fig. 5 is that it is symmetric in α about $\pi/2$. As a consequence, there is a phase with a six-layer repeat in addition to the expected three-layer- and four-layer-repeat structures. This arises as a result of the unrealistically simple and symmetric form chosen in Eqs. (3) and (20) for the short-range interaction $V_{\rm sr}$. The choice of a more realistic short-range potential causes qualitative changes in the form of the phase diagram. For example, strengthening $V_{\rm sr}$ for large α distorts the diagram while maintaining its topology, while modifying the dependence of $V_{\rm sr}$ on $\phi_{l+1}-\phi_l$ can radically change the topology. One choice eliminates the four- and six-layer repeats for certain ranges of η, and allows phase sequences in which one passes from the antiferroelectric Sm-C_A^* phase through the three-layer Sm-C_{FI1}^* phase to the ferroelectric Sm-C^* phase, as is observed in several reported compounds [4]. Another choice eliminates the three- and six-layer repeats for all but a small range of η. If we put

$$V_{\rm sr} = -vL^2(1-\cos\alpha)\sum_l [\cos(\phi_{l+1}-\phi_l-\alpha) + a\cos 3(\phi_{l+1}-\phi_l-\alpha)], \quad (24)$$

then, for $a=0.03$, we find the result shown in Fig. 6(a). The areas representing three- and six-layer repeats are barely visible on this phase diagram, so a magnified detail of this diagram is shown in Fig. 6(b). The dashed line represents the interesting phase sequence Sm-C_A^*–Sm-C_{FI1}^*–Sm-C_{FI2}^*–

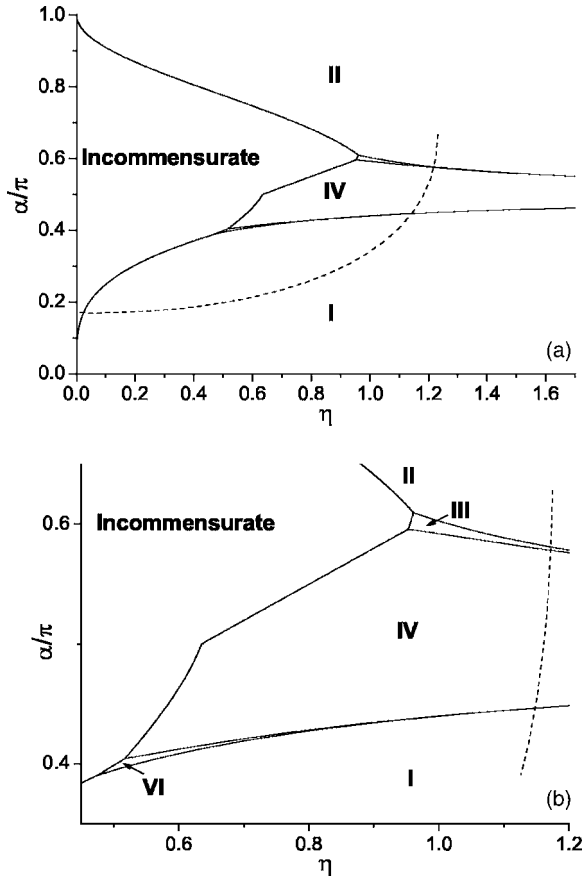

FIG. 6. (a) The phase diagram obtained using the modified short-range interaction suggested in Eq. (24). The dashed line shows the experimentally observed phase sequence for one set of materials. (b) Part of the same diagram enlarged to show details. Here α is in radians.

Sm-C^*–Sm-C^*_α–Sm-A, which has been experimentally observed in some materials [4].

We also note that a material can exhibit different phase sequences depending on its optical purity. The effect of enantiomeric excess on the phase diagram of ferroelectric liquid crystals has been theoretically discussed by Čepič and Žekš [9], and experimentally observed in the compound MHPOBC [20]. At high optical purities, this material passes through the phase sequence shown in Fig. 6. When the optical purity is decreased, however, the intermediate phases disappear and the direct transition between ferro- and antiferroelectric phases is observed. Despite the fact that the long-range interaction discussed in this paper does not depend on such parameters as optical purity and chirality, our mean-field model is capable of producing phase diagrams that depend on such parameters through their effect on the nearest-layer interaction V_{sr}. If, for example, the coefficient a in Eq. (24) is increased to 0.3, then the intermediate phases disappear as shown in Fig. 7, and the phase sequence Sm-C^*_A–Sm-C^*–Sm-A is possible.

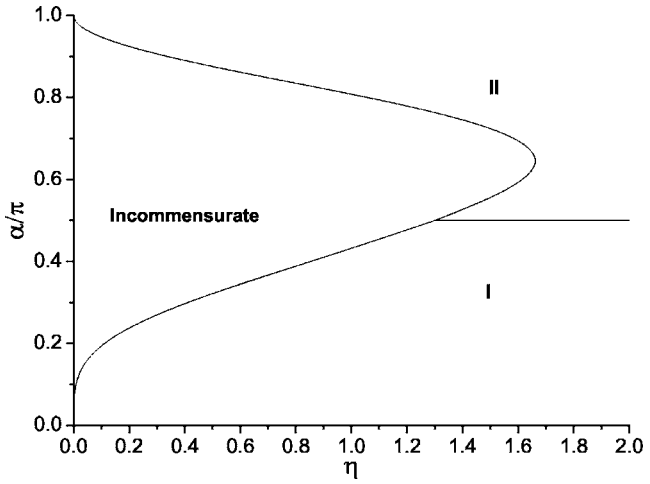

FIG. 7. This figure shows the phase diagram when the parameter a in Eq. (24) is equal to 0.3. This makes possible the direct transition between ferro- and antiferroelectric phases observed in some materials. Here α is in radians.

The principal success of the theory presented above lies in the predicted order in which the phases occur. While the possible choices of V_{sr} are many and arbitrary, the resulting phase sequences are restricted to those that can be traced in a single monotonic line passing across the plot of α as a function of η. No material has been reported, for example, in which a four-layer repeat occurs at a lower temperature than the three-layer repeat, nor has one been found in which the ferroelectric phase occurs at a lower temperature than the four-layer repeat.

V. CONCLUSIONS

We have explored the consequences of including in the free energy of a Sm-C^* liquid crystal the entropy due to thermal fluctuations in the shape of the smectic layers. The anisotropy in the bending elastic constant of a layer leads in a mean-field approximation to a tendency for the c directors in all layers to align in either a parallel or an antiparallel sense. This can be interpreted as an effective long-range interaction between c directors in distant layers. A more exact numerical treatment of the model leads to similar conclusions, but with a reduced strength and range of interaction. The magnitude of the contribution of this effect appears sufficient to induce a variety of commensurate phases. The observed sequences of phases in some recently studied materials are consistent with the sequences permitted by a simple version of the model.

ACKNOWLEDGMENTS

This work was supported by the U.S. National Science Foundation under Grant No. DMR-0072935. We thank C. R. Rosenblatt and R. Pelcovits for valuable comments.

[1] M. B. Hamaneh and P. L. Taylor, Phys. Rev. Lett. **93**, 167801 (2004).
[2] A. D. L. Chandani, E. Gorecka, Y. Ouchi, H. Takezoe, and A. Fukuda, Jpn. J. Appl. Phys., Part 2 **28**, L1265 (1989).
[3] M. Fukui, H. Orihara, Y. Yamada, N. Yamamoto, and Y. Ishibashi, Jpn. J. Appl. Phys., Part 2 **28**, L849 (1989).
[4] L. S. Hirst, S. J. Watson, H. F. Gleeson, P. Cluzeau, P. Barois, R. Pindak, J. Pitney, A. Cady, P. M. Johnson, C. C. Huang, A.-M. Levelut, G. Srajer, J. Pollmann, W. Caliebe, A. Seed, M. R. Herbert, J. W. Goodby, and M. Hird, Phys. Rev. E **65**, 041705 (2002).
[5] Y. Takanishi, K. Hiraoka, V. K. Agrawal, H. Takezoe, A. Fukuda, and M. Matsushita, Jpn. J. Appl. Phys., Part 1 **30**, 2023 (1991).
[6] T. Isozaki, T. Fujikawa, H. Takezoe, A. Fukuda, T. Hagiwara, Y. Suzuki, and I. Kawamura, Phys. Rev. B **48**, 13439 (1993).
[7] Ch. Bahr, D. Fliegner, C. J. Booth, and J. W. Goodby, Phys. Rev. E **51**, R3823 (1995).
[8] M. Čepič and B. Žekš, Mol. Cryst. Liq. Cryst. Sci. Technol., Sect. A **263**, 61 (1995).
[9] M. Čepič and B. Žekš, Phys. Rev. Lett. **87**, 085501 (2001).
[10] P. Mach, R. Pindak, A.-M. Levelut, P. Barois, H. T. Nguyen, C. C. Huang, and L. Furenlid, Phys. Rev. Lett. **81**, 1015 (1998).
[11] J. J. Stott and R. G. Petschek, Phys. Rev. E **60**, 1799 (1999).
[12] P. M. Johnson, D. A. Olson, S. Pankratz, T. Nguyen, J. Goodby, M. Hird, and C. C. Huang, Phys. Rev. Lett. **84**, 4870 (2000).
[13] A. Cady, J. A. Pitney, R. Pindak, L. S. Matkin, S. J. Watson, H. F. Gleeson, P. Cluzeau, P. Barois, A.-M. Levelut, W. Caliebe, J. W. Goodby, M. Hird, and C. C. Huang, Phys. Rev. E **64**, 050702(R) (2001).
[14] D. Konovalov, H. T. Nguyen, M. Čopič, and S. Sprunt, Phys. Rev. E **64**, 010704(R) (2001).
[15] I. Muševič and M. Škarabot, Phys. Rev. E **64**, 051706 (2001).
[16] M. Čepič, E. Gorecka, D. Pociecha, B. Žekš, and H. T. Nguyen, J. Chem. Phys. **117**, 1817 (2002).
[17] P. V. Dolganov, V. M. Zhilin, V. E. Dmitrienko, and E. I. Kats, JETP Lett. **76**, 498 (2002).
[18] P. V. Dolganov, V. M. Zhilin, V. K. Dolganov, and E. I. Kats, Phys. Rev. E **67**, 041716 (2003).
[19] D. A. Olson, X. F. Han, A. Cady, and C. C. Huang, Phys. Rev. E **66**, 021702 (2002).
[20] E. Gorecka, D. Pociecha, M. Čepič, B. Žekš, and R. Dabrowski, Phys. Rev. E **65**, 061703 (2002).
[21] R. Bruinsma and J. Prost, J. Phys. II **4**, 01209 (1994).
[22] A. Ajdari, L. Peliti, and J. Prost, Phys. Rev. Lett. **66**, 1481 (1991).
[23] N. Uchida, Phys. Rev. Lett. **87**, 216101 (2001).
[24] P. Ziherl, R. Podgornik, and S. Zumer, Phys. Rev. Lett. **82**, 1189 (1999).
[25] Orsay Liquid Crystal Group, Solid State Commun. **9**, 653 (1971).
[26] A. Cady, D. A. Olson, X. F. Han, H. T. Nguyen, and C. C. Huang, Phys. Rev. E **65**, 030701(R) (2002).
[27] T. Carlsson, I. W. Stewart, and F. M. Leslie, Liq. Cryst. **9**, 661 (1991).
[28] A. B. Pippard, Eur. J. Phys. **8**, 55 (1987).
[29] P. L. Taylor and O. H. Heinonen, *A Quantum Approach to Condensed Matter Physics* (Cambridge University Press, Cambridge, U.K., 2002).
[30] A. Findon and H. F. Gleeson, Ferroelectrics **277**, 35 (2002).
[31] T. Kontorova and Y. I. Frenkel, Zh. Eksp. Teor. Fiz. **8**, 89 (1938).
[32] A. Banerjea and P. L. Taylor, Phys. Rev. B **30**, 6489 (1984).
[33] M. Mehta, Phys. Lett. A **252**, 288 (1999).
[34] B. Chirikov, Phys. Rep. **52**, 265 (1984).
[35] J. F. Li *et al.*, Jpn. J. Appl. Phys., Part 2 **35**, L1608 (1996).
[36] J. F. Li, X. Y. Wang, E. Kangas, P. L. Taylor, C. Rosenblatt, Y. I. Suzuki, and P. E. Cladis, Phys. Rev. B **52**, R13075 (1995).
[37] J. P. F. Lagerwall, P. Rudquist, S. T. Lagerwall, and F. Giebelmann, Liq. Cryst. **30**, 399 (2003).
[38] D. A. Olson, S. Pankratz, P. M. Johnson, A. Cady, H. T. Nguyen, and C. C. Huang, Phys. Rev. E **63**, 061711 (2001).
[39] G. Hepke, D. Lötzsch, J. Bömelburg, and S. Rauch, Mol. Cryst. Liq. Cryst. Sci. Technol., Sect. A **317**, 65 (1998).
[40] T. Isozaki, T. Fujikawa, H. Takezoe, and A. Fukuda, Ferroelectrics **147**, 121 (1993).